

## TIME-DEPENDENT WAVEPACKET CALCULATIONS OF ATOM SCATTERING FROM SURFACES WITH IMPURITIES

A.T. YINNON, R. KOSLOFF and R.B. GERBER

*Department of Physical Chemistry and The Fritz Haber Research Center for Molecular Dynamics,  
The Hebrew University of Jerusalem, Jerusalem 91904, Israel*

Received 13 December 1983

Exact quantum-mechanical calculations are reported on atom scattering from a crystalline surface with isolated impurities. The calculations are for He scattering from a one-dimensional model of a Cu surface with adsorbed Ar atoms. The difficulties of carrying out calculations on scattering from extended but non-periodic structures are overcome by using a time-dependent wavepacket approach. A recently developed method for solving the time-dependent Schrodinger equation is employed. Scattering intensities are given for several energies and incidence angles. Detailed insight is obtained on impurity effects on surface scattering. The main features are: (1) Broad intensity tails are superimposed on each diffraction spike. The width of the tails decreases with increasing diffraction order; (2) Shallow rainbow peaks arise, due to impurity induced local corrugation; (3) Weak intensity maxima arise due to interference between surface and impurity scattering. The intensities are somewhat sensitive to the position of the impurity within the surface unit cell. Physical interpretation of the effects is provided from exact calculations, and from a simple sudden approximation for the scattering intensities. It is argued that He scattering can be used to determine impurity locations on surfaces.

### 1. Introduction

The study of impurities and imperfections in crystalline surfaces is of considerable fundamental interest and has potentially significant applications. Every real surface contains impurities and defects to some extent. Many surface systems of chemical importance, e.g., most practical catalysts [1], contain substantial amounts of impurities and defects which greatly affect their performance. Since structure may be the key for understanding many of the properties of these systems, there is strong motivation for pursuing methods for structural characterization of imperfect surfaces. One of the most powerful structural probes of crystalline surfaces is scattering of He atoms [2-7]: at moderate experimental energies, the atoms do not penetrate beyond the surface layer, and also, the scattering pattern is sensitive to local structural features. For the very same reasons, He scattering appears potentially to be an attractive choice for probing imperfect or disordered surfaces. Very little is known so far on scattering from imperfect

surfaces, either experimentally or theoretically. Previous theoretical studies on effects of disorder or defects on scattering from surfaces [8-11] were nearly all confined by method to special imperfection models (e.g., random steps [9,11]). Furthermore, virtually all published studies seem to employ approximations for the scattering dynamics [9-11] the validity of which was not yet established. Most recently exact results were announced by the present authors [12] and, independently, by Drolshagen and Heller [13] on atom scattering from imperfect surfaces. The results are exact in the sense that they represent a converged numerical solution of the scattering equations for a specific imperfect, rigid surface model. In both cases [12,13] the methods used involved an algorithm for solving the time-dependent Schrödinger equation, and a description of the process in terms of wavepacket scattering.

The purpose of the present article is to present more extensive exact calculations for He scattering from a crystalline surface with an adsorbed atom impurity, within the framework of a rigid surface

model. The main focus will be on two questions: (1) How do dilute impurities (in the isolated defect limit) affect the scattering intensity features; (2) is the scattering pattern significantly sensitive to impurity location, i.e., can one expect experimental intensities to yield information on impurity positions. The material is presented as follows: section 2 describes the model system used, including surface structural parameters and interaction potentials. Section 3 outlines the numerical method used for solving the time-dependent Schrödinger equation. Section 4 presents the results, and provides an analysis of the main impurity effects on the scattering pattern. Concluding remarks are brought in section 5.

## 2. The model

The system considered here is a very simplified representation of low-concentration atomic impurities adsorbed on a crystalline surface. The solid surface will be assumed to be completely rigid, and the impurities will likewise be taken as vibrationless, held in fixed positions. While surface and impurity vibrations do certainly affect scattering intensities, a rigid surface model should provide at least a useful starting point in studying the realistic problem. (In the case of pure crystalline surfaces, phonon effects are most practically introduced through Debye-Waller [14] factors, and a similar approximate approach may be possible for the present system also.) To simplify further the computational effort involved, a one-dimensional model surface will be treated. While crude, such models frequently yield reasonable results when applied to the analysis of the in-plane scattering [14], i.e. collisions where the incident and the final momenta lie in the same plane, the latter being perpendicular to the surface lattice. The one-dimensional surface model should naturally be taken with structural parameters pertaining to those of the corresponding real surface, along its intersection with the collision plane. When applied to a real system, such a one-dimensional model obviously neglects out-of-plane scattering, that may be important for surfaces of high corrugation. Calculations for realistic two-dimensional surfaces are

presently at early stages of progress. We consider here scattering at relatively high energies in the direction perpendicular to the surface, in which case the short-range repulsive interactions dominate the collision. Note further that impurities were assumed to be extremely dilute, hence  $d_1 \gg \alpha_1^{-1}$ , where  $d_1$  is the average inter-impurity distance, and  $\alpha_1^{-1}$  the range scale of impurity atom interaction with the incoming He atom. A given collision will then be influenced by one impurity atom at most in addition to the underlying surface. The interaction potential experienced by the He atom will be taken in the form:

$$V(x, z) = V_s(x, z) + V_1 \left[ (x - x_1)^2 + (z - z_1)^2 \right]^{1/2}, \quad (1)$$

where  $x_1, z_1$  are the coordinates of the (only) impurity located within the interaction range of the He atom.  $z$  is the distance of the He from the surface plane and  $x$  is the coordinate of the He along the surface direction. Within the additive interaction model (1),  $V_s(x, z)$  is the potential between He and the crystalline surface involved,  $V_1(x, z)$  – the He/impurity atom interaction. Taking Ar as the adsorbed atom, a Morse potential model was employed for the He/Ar interaction, with well-depth and with range parameters that were taken from gas-phase data [15]. The interaction between the crystalline surface and the He atom was modelled by a Lennard-Jones– Devonshire potential function [14]:

$$V_s(z, x) = D(e^{-2\alpha z} - 2e^{-\alpha z}) + \beta D e^{-\alpha z} \cos(2\pi x/a). \quad (2)$$

The values of most parameters in (2) were taken so as to correspond roughly to the case of low Miller index faces of Cu [7,16] (e.g., Cu(110), Cu(100)). The lattice constant was taken as 4.8378 bohr, as for Cu(100) [16]. Potential parameters for the He/Cu(100) interaction were determined by Armand et al. [7] from diffraction scattering, and the steepness and well-depth parameter values in the case of He/Cu(100) are believed to be quite similar [16]. On that basis, we chose  $\alpha = 0.6 \text{ bohr}^{-1}$ ,  $D = 0.000234 \text{ hartree}$ . To illustrate the effects of the impurity on the diffraction pattern, we found

it useful to carry out calculations for two values of  $\beta$ : The case of a non-corrugated surface model  $\beta = 0$ , and the case of  $\beta = 0.05$  which is higher than found for the low-index faces of Cu [7], and hence offers more pronounced diffraction lines, making the impurity effects easier to identify. It is probably realistic to expect all smooth metal faces to correspond to  $\beta < 0.05$ , and the comparison between the non-corrugated, and the (relatively) rough surface result offers insight pertinent to any intermediate case. To examine the sensitivity of the scattering to impurity location, calculations were carried out, both for impurity at site  $x_1 = 0$  within the unit cell (on top of a Cu atom of the underlying surface), and for impurity at site  $x_1 = a/2$  within the unit cell (impurity placed between two neighbouring Cu atoms). The distance  $z_1$  of the Ar impurity from the surface plane was set as follows. Denoting by  $z = 0$ , the position determined by the line through the centers of the Cu atoms, the "on top" position of Ar corresponds to  $z_1 = 6.0$  bohr (from the atomic radii of Cu and Ar). Similarly geometry suggests that for the "in between" positions  $z_1 = 4.8$  bohr is reasonable.

### 3. Method and calculations

The basis of the method employed here is a recently proposed algorithm [16,17] for solving the time-dependent Schrödinger equation:

$$i\hbar\partial\Psi(\mathbf{r}, t)/\partial t = [-(\hbar^2/2m)\nabla_r^2 + V(\mathbf{r})]\Psi(\mathbf{r}, t). \quad (3)$$

The algorithm was described in detail elsewhere [17,18] and applied to gas-phase molecular collisions [18] and to scattering from crystalline surfaces [19]. Only a brief description of the scheme will be given here. To obtain the time-evolution of a wavepacket from an initial state by time-propagation processes on eq. (3) requires efficient calculations of  $H\Psi(\mathbf{r}, t)$  for every space point  $\mathbf{r}$  at each time step  $t$ . A major difficulty in this respect is the need for fast and accurate evaluations of the second-order derivatives  $\nabla_r^2\Psi(\mathbf{r}, t)$ . In the present scheme this is carried out as follows. A fast-Fourier transform algorithm is used to transform  $\Psi(\mathbf{r}, t)$

into  $k$  space, yielding a function  $\tilde{\Psi}(\mathbf{k}, t)$ . The action of  $\nabla^2$  in  $k$  space is represented by multiplication by  $-k^2$ . The result is then back-transformed into  $\mathbf{r}$  space by a second application of the FFT routine, yielding  $\nabla_r^2\Psi(\mathbf{r}, t)$ . Symbolically, one has:

$$\Psi(\mathbf{r}, t) \xrightarrow{\text{FFT}} \tilde{\Psi}(\mathbf{k}, t) \rightarrow -k^2\tilde{\Psi}(\mathbf{k}, t) \xrightarrow{\text{FFT}} \nabla_r^2\Psi(\mathbf{r}, t). \quad (4)$$

The effectiveness of the procedure depends essentially on the efficiency and accuracy of the FFT technique. In this method, numerical effort increases as  $O(N \log N)$ , where  $N$  is the number of grid points in  $\mathbf{r}$  space.

To propagate the wavepacket in time, second-order differentiating is employed: denoting by  $t_n$  the  $n$ th time point, and setting  $\Psi^n(\mathbf{r}) \equiv \Psi(\mathbf{r}, t_n)$  the time derivative in eq. (3) is approximated by

$$[\partial\Psi(\mathbf{r}, t)/\partial t]_{t=t_n} = (1/2\Delta t)[\Psi^{(n+1)}(\mathbf{r}) - \Psi^{(n-1)}(\mathbf{r})], \quad (5)$$

where  $\Delta t$  is the interval between successive time points. The approximation (5) is of second-order accuracy. The time-dependent Schrödinger equation now becomes

$$\Psi^{(n+1)} = \Psi^{(n-1)} - 2i\Delta t H\Psi^{(n)}. \quad (6)$$

The overall process of solution is the following one: For given  $n$ , assuming  $\Psi^{(i)}$  for  $i = 0, \dots, n$  is available from previous steps,  $H\Psi^{(n)}$  is calculated by the FFT-based algorithm described in (4).  $\Psi^{(n+1)}$  is computed from (6), and the process is continued for  $\Psi^{(i)}$ ,  $i > n + 1$ , till the solution has been obtained for sufficiently long times. To initiate the above process, both  $\Psi(\mathbf{r}, t_0)$  and  $\Psi(\mathbf{r}, t_1)$  are needed as input, while the Schrödinger equation (3) requires only  $\Psi(\mathbf{r}, t_0)$  to determine a unique solution, and only a single-time initial condition is generally available from physical considerations. This is overcome by using first a single step of Runge-Cutta integration to generate  $\Psi(\mathbf{r}, t_1)$  from  $\Psi(\mathbf{r}, t_0)$  according to eq. (3). Further details are given in refs. [16,17].

In the present problem  $\mathbf{r} = (x, z)$ , with  $x$  the coordinate parallel to the surface and  $z$  perpendic-

ular to that direction. The initial state was taken at a pre-collision time  $t_0$  ( $t_0 \rightarrow -\infty$ ), as an extended wave in the  $x$  direction and a localized packet along  $z$ :

$$\Psi(z, x, t_0) = \exp(ik_x x) \exp[ik_z(z - z_0)] \times \exp[-A(z - z_0)^2], \quad (7)$$

where  $\hbar k_x$ ,  $\hbar k_z$  are, respectively, the momentum in the  $x$  direction and the (mean) momentum in the  $z$  direction,  $z_0$  was taken to be far outside the He-surface interaction range. Essentially, the integration thus begins at  $t_0 \rightarrow -\infty$  with a wavepacket at distance  $z_0 \rightarrow \infty$  from the surface plane. In principle, the results obtained with an initial wavepacket such as (7) should be transferred to correspond to the usual plane-wave incoming conditions of scattering theory. However, a small value of the parameter  $A$  ( $\frac{1}{2}$  bohr $^{-2}$ ) in eq. (7) was used, so that the  $z$ -dependence of the wavepacket was almost that of a delocalized wave, and it was tested and found numerically that transformation of the results is unnecessary. All the calculations reported here correspond to incidence normal to the surface ( $k_x = 0$ ). At the relatively high energies normal to the surface for which the calculations were done, scattering is dominated by the repulsive forces. Influence of the impurity on the wavepacket is thus short range. It was possible therefore to confine the calculation in the  $x$  coordinate to an interval  $[x_1 - L, x_1 + L]$  around the impurity center  $x_1$  where the interval  $2L$  included 12 unit cells of the underlying Cu surface. The solution  $\Psi(x, z, t)$  outside that interval can be obtained by periodicity in the  $x$  variable that holds to excellent accuracy at distances sufficiently far from the impurity site (starting already from points within the edge unit cells inside the interval). Calculations were initiated at  $t = t_0 \rightarrow -\infty$  with  $z_0$  for outside the interaction range, and propagated to sufficiently large  $t$  ( $t \rightarrow \infty$ ) when the wavepacket after the collision has propagated to such distances from the surface that the interaction becomes negligible and asymptotic behaviour has been attained. The scattering intensities were extracted from the asymptotic, post-scattering values of the solution. The scattering intensity into final

$(k'_x, k'_z)$  satisfies:

$$I_{k_x, k_z \rightarrow k'_x, k'_z} \propto \left| \iint \exp(-ik'_x x) \exp(-ik'_z z) \times \Psi(x, z, t \rightarrow \infty) dx dz \right|^2. \quad (8)$$

In addition, considerable insight into the dynamics was obtained from finite time values of the wavepacket: All calculations were carried out on the VAX 750/11 of the Fritz Haber Center at the Hebrew University of Jerusalem. Calculations were carried out for collision energies 0.000315 and 0.000659 hartree, in both cases at normal incidence. Computing time was  $\approx 100$  min per scattering event.

## 4. Results and analysis

### 4.1. Main impurity effects on the scattering

Fig. 1 shows the scattering intensities as a function of the momentum transfer  $\Delta k_x = k'_x - k_x$  parallel to the surface for He scattered from [Cu(surface) + Ar(impurity)] at collision energy 0.000315 hartree. The corrugation parameter of the Cu surface in this calculation is  $\beta = 0.05$ . It is instructive to compare the results with those of fig. 2 showing intensities for He scattering from a

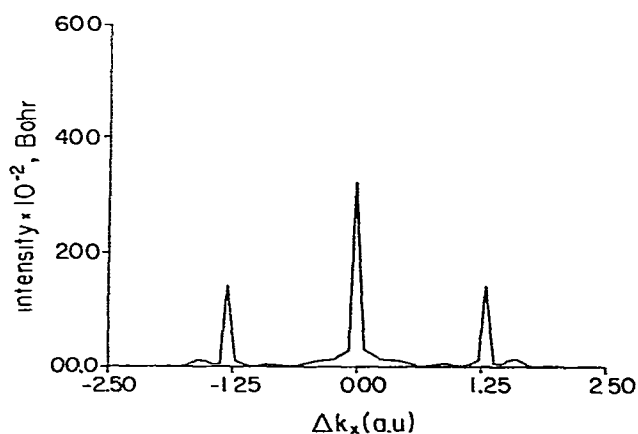


Fig. 1. Intensity distribution for He scattered from [Cu(surface) + Ar(impurity)]. The results are for Ar position between neighbouring Cu surface atoms (coordinates  $x_1 = a/2$ ,  $z_1 = 4.8$  bohr). [Cu surface corrugation parameter is  $\beta = 0.05$ .] Collision energy is 0.000315 hartree.

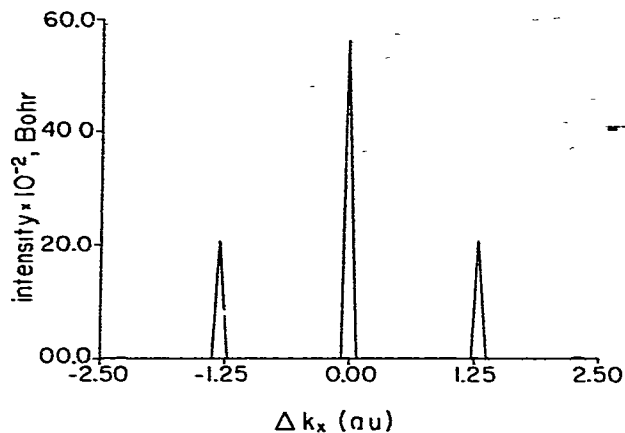


Fig. 2. Intensity distribution for He scattered from a pure-crystal line Cu surface. The width of the diffraction spikes shown is strictly numerical. A surface corrugation parameter  $\beta = 0.05$  was used. Collision energy is 0.000315 hartree.

corresponding impurity-free Cu surface. The pure crystalline case obviously gives rise to unperturbed diffractive scattering, and fig. 2 shows a specular peak, and two symmetric first-order diffraction peaks at  $\Delta k_x = \pm 2\pi/a$  where  $a$  is the lattice constant of the Cu surface. The width of the diffraction spikes in fig. 2 is strictly numerical in origin, related to the grid-size employed in  $k$  space. Fig. 1 shows that the contaminated surface system gives rise to diffraction spikes at the same positions as the pure surface. The intensity patterns of the pure and the contaminated surface differ, however, in three major aspects: (i) The scattering from the Cu + Ar (impurity) system gives rise to broad intensity tails superimposed on the diffraction spikes. The intensity tails around the specular peak are particularly broad, with a halfwidth of  $(\Delta k)_{\text{wid}} \approx 0.4 \text{ bohr}^{-1}$ . The tails of the first-order diffraction peaks are weaker, but include a non-negligible fraction of the intensity of the diffraction spike. The fact that scattering from imperfect surfaces gives rise to intensity tails around the diffraction spots has been observed in previous studies [8–11]. (ii) The impure surface gives rise to two intensity maxima, placed symmetrically at  $(\Delta k_x) = \pm 1.625 \text{ bohr}^{-1}$ , beyond the observed diffraction spikes, which do not occur for the pure crystalline surface. (iii) A second pair of symmetric shallow peaks are

present in the intensity spectrum of the contaminated surface, without a corresponding feature in the pure crystalline case. The second pair of impurity-induced peaks are located between the specular and the first-order diffraction spikes, at  $\Delta k_x = \pm 0.875 \text{ bohr}^{-1}$ , and are weaker than the maxima at  $\pm 1.625 \text{ bohr}^{-1}$ . The impurity-induced maxima of the types (ii) and (iii) were first reported in a preliminary announcement of the present results [12]. Another aspect, rather obvious physically but important to note, is that the presence of the impurity results in decrease of the total coherent scattering, as represented by the *diffraction spikes*. As comparison of fig. 1 with fig. 2 shows, even for the dilute impurity case described by the present model system the decrease of coherent scattering is of observable magnitude, as it must be, to account for the flux scattered into the *diffraction tails*, and by the impurity-induced maxima, which together constitute the incoherent scattering. We proceed now to analyze the new features of impurity-induced scattering.

#### 4.2. Interpretation of the main impurity effects

The fact that various types of crystalline imperfection give rise to intensity tails superimposed on the diffraction spikes has been previously observed in approximate calculations on scattering from disordered solids [8–11]. Qualitatively, the following general argument can be made. Diffraction spikes arise in scattering from a perfectly crystalline surface, since constructive interference comes from scattering at some equivalent sites on different unit cells, while interference from non-equivalent sites on different cells leads to destructive interference. For a non-crystalline solid, the constraints on constructive interference are relaxed. In the present case, components of the wavepacket scattered from the Cu surface involved, which correspond to a non-Bragg value of  $\Delta k_x$ , may interfere with a component scattered from the impurity, and yield finite intensity. The “compensating” effect of scattering from the impurity site that leads to some constructive interference for non-Bragg scattering from the surface, is expected to be weaker the more incoherent is the wave emerging from the Cu array. Hence the decay of

the intensity tails as  $\Delta k_x$  deviates considerably from the diffraction values  $2\pi n/a$ . To interpret the new, impurity-induced maxima described in section 4.1, we consider fig. 3 showing scattering intensities for the same He/[Cu(surface) + Ar(impurity)] systems as in section 4.1, except that here a non-corrugated Cu surface ( $\beta=0$ ) was employed. Comparison of fig. 1 with fig. 3 shows that the impurity-induced maxima are approximately independent of the corrugation of the underlying Cu surface, and can in fact be quantitatively accounted for by a model involving an impurity on an otherwise flat surface. Examination of the detailed wavepacket solution suggests that the peaks at  $\Delta k_x = \pm 1.625 \text{ bohr}^{-1}$  are due to the strong local corrugation introduced by the impurity as given by  $V_1(x, z)$ . The much shallower maxima, at lower momentum transfer of  $\Delta k_x = \pm 0.875 \text{ bohr}^{-1}$ , are due to interference between the wave reflected from the surface and that scattered from the impurity. The maxima at low momentum transfer are therefore sensitive to the impurity distance from the surface plane [ $z_1$  in eq. (1)]. It should be noted that the impurity-induced tails of the diffraction peaks are sensitive also to  $x_1$ , the impurity location within the unit cell. We conclude that experimental determination of the impurity induced features in the intensity pattern could yield detailed information on impurity location with respect to the underlying surface.

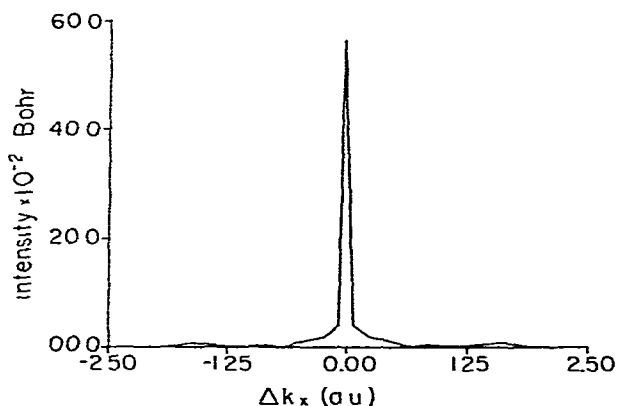


Fig. 3. Intensity distribution for He scattered from an Ar impurity on a flat surface. The impurity center is at  $z_1 = 60$  bohr from the (non-corrugated) surface plane. Collision energy is 0.000315 hartree.

It should be very desirable to be able to study the impurity-induced effects in terms of simple models. We wish to suggest here that in view of its convenience of interpretation, the *sudden approximation* [10,20] may prove very useful in this respect. This approximation, introduced first for diffractive scattering from pure crystalline systems [20], was recently applied to scattering from disordered surfaces [10]. It is an impulse collision approximation that assumes momentum transfer due to corrugation, parallel to the surface, to be considerably smaller than the momentum transfer perpendicular to the surface:

$$k_z \gg \Delta k_x. \quad (9)$$

The energies at which the calculations reported here were carried out are not sufficiently high for the sudden approximation to hold quantitatively, but it can probably be relied upon for gaining qualitative insight. In the present case, the sudden approximation gives the following expression [10] for  $I(\Delta k_x)$  parallel to the surface:

$$I(\Delta k_x) \propto \left| \frac{1}{L} \int_{-L}^L \exp(i\Delta k_x x) \exp[2i\eta(x)] dx \right|^2, \quad (10)$$

$$L \rightarrow \infty,$$

where  $\eta(x)$  is the phase shift given by:

$$\eta(x) = \int_{z_1}^{\infty} \left\{ [k_z^2 - (2m/\hbar^2)V(x, z)]^{1/2} - k_z \right\} dz - k_z z_1, \quad (11)$$

where  $z_1$  is the classical turning point corresponding to the integrand in (11). In the flat surface model for the underlying Cu,  $V(x, z) = V_s(z) + V_1(x, z)$ . Assume that, as in the present example, the corrugation at the vicinity of the impurity is strong, i.e.  $V_1(x, z)$  varies rapidly with  $x$ , and so will  $\eta(x)$  also. A stationary-phase evaluation of (10) should then be applicable, yielding:

$$I(\Delta k_x) \propto \left[ \partial^2 \eta(x) / \partial x^2 \right]_{x=x_s}^{-1}, \quad (12)$$

where the stationary-phase point  $x_s$  is given by:

$$\Delta k_x = - \left[ \partial \eta(x) / \partial x \right]_{x=x_s}. \quad (13)$$

Eq. (12) suggests the occurrence, in the crude

stationary phase limit (12), of a rainbow in the scattering intensity due to the impurity corrugation. We suggest on the basis of preliminary calculations that the impurity-induced peaks at large momentum transfer ( $\Delta k_x = \pm 1.825 \text{ bohr}^{-1}$ ) in fig. 1 correspond to this interpretation, although the exact quantum calculation gives a finite maximum unlike the singularity of the crude stationary-phase limit (as is always the case for rainbow effects [21]). Detailed sudden interpretations of impurity-induced intensity features, as well as quantitative calculations with that method at high energies, are in progress [22].

#### 4.3. Dependence of scattering intensities on impurity location

The same calculations as described in section 4.1 were carried out also for a slightly different system with the Ar impurity "on top" of a surface Cu atom (position  $x_1 = 0$ ,  $z_1 = 6.0 \text{ bohr}$  within the unit cell), instead of the position between two neighbouring Cu atoms ( $x_1 = a/2$ ,  $z_1 = 4.8 \text{ bohr}$ ) in the previous case. The results for the new configuration are shown in fig. 4. Comparison with fig. 1 shows that impurity effects on the scattering are stronger for the new configuration. In particular, while in fig. 1, the intensity tails fall off smoothly and rapidly with the distance of  $\Delta k_x$

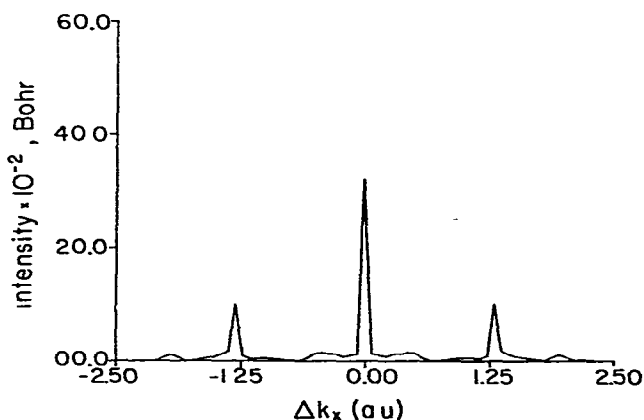


Fig. 4. Intensity distribution for He scattered from [Cu(surface) + Ar(impurity)]. Results are for Ar position on top of a Cu surface atom ( $x_1 = 0$ ,  $z_1 = 6.0 \text{ bohr}$ ). Other details are as in fig. 1.

from the Bragg values, impurity effect on the near-specular scattering in the case of fig. 4 is strong enough to produce shoulders with off-specular maxima at  $\Delta k_x \approx \pm 0.45 \text{ bohr}^{-1}$ . Also, the total intensity in the impurity induced background around the specular peak is larger in fig. 4 than in fig. 1. The "on top" impurity configuration induces also more pronounced intensity tails at the first-order diffraction peaks than is found in fig. 1. Finally, we note that the pair of impurity-induced maxima found in the case of fig. 1 at  $(\Delta k_x) = \pm 0.825 \text{ bohr}^{-1}$  occur in fig. 4 at somewhat larger values of momentum transfer, indicative of greater corrugation. Indeed, all the differences between fig. 1 and fig. 4 can be readily explained on the basis of geometry, the Ar placed on top of a Cu atom ( $x_1 = 0$ ,  $z_1 = 6.0 \text{ bohr}$ ) leads to a substantially more corrugated structure than the same impurity when located between two neighbouring Cu atoms ( $x_1 = a/2$ ,  $z_1 = 4.8 \text{ bohr}$ ) and partly shielded by the latter. The most important conclusion from the comparison of fig. 1 and fig. 4 is that the scattering intensities are sensitive to impurity location, on a scale that should probably make it possible to extract information on impurity position from experimental data

#### 4.4. Energy-dependence of impurity effect on the scattering

Fig. 5 shows the scattering intensity versus  $\Delta k_x$  for He/[Cu(surface) + Ar(impurity)] at collision energy  $0.000659 \text{ hartree}$ . As in fig. 1, impurity location is  $x_1 = a/2$  (i.e. between the centers of two neighbouring Cu atoms),  $z_1 = 4.8 \text{ bohr}$ . In fig. 5 the second-order diffraction peaks  $\Delta k_x = \pm 4\pi/a$  are also seen. This is, of course, an effect pertinent to the crystalline layer involved and a consequence of the fact that the effective corrugation increases with increasing incidence energy normal to the surface as the He probes shorter-range parts of the interaction  $V(x, z)$  where the coupling is stronger. Impurity effect on the specular peak is somewhat stronger in the high-energy case of fig. 5 than in fig. 1: The impurity-induced intensity around the specular spike has, in fig. 5, the form of a flat broad maximum rather than a monotonic fall-off with  $\Delta k_x$ . Clearly, also the contribution of the

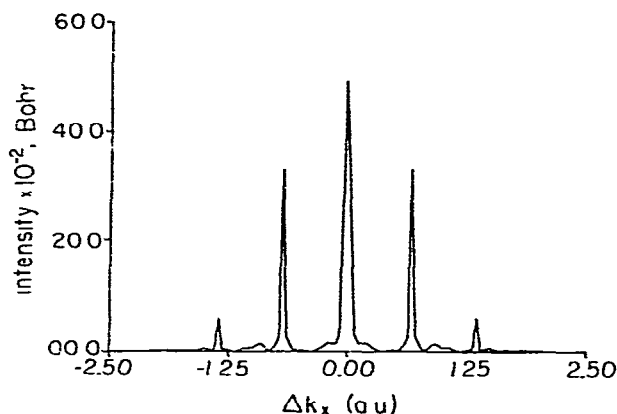


Fig. 5 Intensity distribution for He scattered from [Cu(surface) + Ar(impurity)]. Results are for a collision energy of 0.000659 hartree. All other details are as in fig. 1.

impurity to the effective corrugation increases with the energy, again for the reason that at higher incidence energy the projectile probes distances nearer to the center of the impurity where  $V_1(x, z)$  involves stronger coupling between the  $z$  and the  $x$  motions. As in fig. 1, two types of impurity-induced maxima are seen outside the diffraction spikes. The furthest of these, at  $\Delta k_x = \pm 2.88 \text{ bohr}^{-1}$ , pertain to much greater momentum transfer than the corresponding outer peaks in the low-energy case, which is another manifestation of the increase with energy of effective corrugation due to the impurity. The pair of impurity-induced intensity structures, with maxima at  $\Delta k_x = \pm 1.48 \text{ bohr}^{-1}$  seem (by analysis of the wavepacket solution) to be a consequence of interference between scattering from the impurity and scattering from the surface. The increased intensity of these peaks (compared with the corresponding maxima at  $\Delta k_x = \pm 0.875 \text{ bohr}^{-1}$  in fig. 1) shows that with increased effective corrugation contributed by both the Cu surface and the impurity, the off-specular constructive interference is enhanced. For a pure crystalline surface, increase of energy yields more diffraction peaks and may thus render more structural information on the surface. The above results give rise to an analogous conclusion for an impurity-doped crystal – some of the impurity effects on the scattering become more pronounced with the increase of collision energy.

In analyzing the results obtained from the model it is important to bear in mind the question of the correspondence of the system studied to realistic impure surface systems. One important aspect is that adsorbed impurities on real surfaces may be distributed over several types of sites. The present model assumes a single type of site for each impurity with the unit cell, and is therefore an idealized limit, approached only in cases where such a single site is energetically overwhelmingly favoured. Also, the present model is confined to calculations on a finite cluster (of 12 unit cells) with periodic boundary conditions imposed at the edges. The intensities as given thus represent a system with a one-dimensional coverage ratio of 1(Ar):12 (underlying Cu unit cells). For lower impurity concentrations, the coherent part of the scattering (i.e. the diffraction spikes) scales with the number of undeveloped unit cells, while the incoherent scattering intensities (diffraction tails, impurity-induced maxima) decrease correspondingly. Our results can therefore be adequately scaled to any impurity concentration lower than the 1:12 ratio. Such a scaling cannot be applied in the regime of higher concentration, since in this case interference effects between neighbouring impurities may become significant.

## 5. Concluding remarks

In this article, exact quantum-mechanical calculations were reported on scattering of He from a model system representing an impurity atom adsorbed on a crystalline surface. The calculations were confined to the framework of a rigid, vibrationless surface, and to a one-dimensional surface model. The interaction and structural parameters employed in the calculations are probably realistic, at least qualitatively. The main result of the calculations has been to demonstrate several important qualitative effects in the scattering due to the presence of the impurity, including intensity tails for the diffraction peaks and several new maxima related to scattering from to impurity, and to interference between scattering from surface and from the impurity. An important aspect of the results is the finding that the intensity pattern is

reasonably sensitive to impurity location. This suggests strongly that the He scattering could prove a useful crystallographic probe of impurities on surfaces, leading, in combination with calculations such as presented here to determination of impurity position on the surface. We hope this will provide strong motivation for experimental efforts in this area. At the same time it seems desirable to develop further the theory, in particular with regard to a search for further new effects in other types of imperfect crystal systems.

### Acknowledgement

The Fritz Haber Center is supported by the Minerva Gesellschaft für die Forschung, Munich, Federal Republic of Germany. RK acknowledges support by a grant from the Foundation of Basic Research of the Israel Academy of Sciences.

### References

- [1] G.A. Somorjai, *Chemistry in two dimensions surfaces* (Cornell Univ. Press, Ithaca, 1981)
- [2] T. Engel, *Israel J. Chem.* 22 (1982) 294.
- [3] T. Engel and K.H. Reider, in: *Structural studies of surfaces*, ed. G. Hohler (Springer, Berlin, 1981).
- [4] A. Lebsch and J. Harris, *Surface Sci.* L111 (1981) 721.
- [5] R.B. Laughlin, *Phys. Rev.* B25 (1982) 222.
- [6] A. Tuschida, *Surface Sci.* 46 (1974) 611.
- [7] G. Armand, J. Lapujoulade, J.R. Manson, J. Perreau and B. Salanon, *Israel J. Chem.* 22 (1982) 298.
- [8] J.M. Cowley and H. Schuman, *Surface Sci.* 38 (1973) 53.
- [9] J. Lapujoulade, *Surface Sci.* 108 (1981) 526.
- [10] J.I. Gersten, R.B. Gerber, D.K. Dacol and H. Rabitz, *J. Chem. Phys.* 78 (1983) 4277.
- [11] G.E. Tommei, A.C. Levy and R. Spadacini, *Surface Sci.* 125 (1983) 312.
- [12] R.B. Gerber, A.T. Yinnon and R. Kosloff, *Chem. Phys. Letters* 105 (1984) 523.
- [13] G. Drolshagen and E.J. Heller, to be published.
- [14] F.O. Goodman and H.Y. Wachman, *Dynamics of gas-surface scattering* (Academic Press, New York, 1976)
- [15] U. Buck, *Advan. Chem. Phys.* 30 (1975) 314
- [16] J. Perreau and J. Lapujoulade, *Surface Sci.* 119 (1982) 181.
- [17] D. Kosloff and R. Kosloff, *J. Comput. Phys.* 52 (1983) 35.
- [18] R. Kosloff and D. Kosloff, *J. Chem. Phys.* 79 (1983) 1823.
- [19] A.T. Yinnon and R. Kosloff, *Chem. Phys. Letters* 102 (1983) 216
- [20] R.B. Gerber, A.T. Yinnon and J.N. Murrell, *Chem. Phys.* 31 (1978) 1;  
R.B. Gerber and A.T. Yinnon, *J. Chem. Phys.* 73 (1980) 5363
- [21] M.S. Child, *Molecular collision theory* (Academic Press, New York, 1974)
- [22] R.B. Gerber and A.T. Yinnon, to be published